Internal micropulse structure of a storage-ring free-electron laser

G. De Ninno,[1,2] D. Nutarelli,[3] D. Garzella,[1,2] and M. E. Couprie[1,2]
[1]*CEA/DSM/DRECAM, Gif-sur-Yvette, France*
[2]*LURE, Orsay, France*
[3]*LAC, Orsay, France*
(Received 5 June 2001; published 17 May 2002)

The longitudinal distribution of a free-electron laser (FEL) may present a complex internal structure. This phenomenon has been already observed in the case of LINAC based oscillators and self-amplified spontaneous emission devices (for which the presence of ''spikes'' in the temporal distribution is systematically observed). We investigate here the physical process responsible for the growth of complex substructures inside the micropulse of a storage-ring free-electron laser. This ''hole-burning-like'' process results from the localized character of the interaction between the ultrarelativistic electron beam circulating in the storage ring and the laser pulse. Experimental results concerning the case of the super-ACO FEL are presented and interpreted by means of a pass-to-pass tracking code containing all the relevant features of the system dynamics.

DOI: 10.1103/PhysRevE.65.056504 PACS number(s): 41.60.Cr, 29.20.Dh

I. INTRODUCTION

The free-electron laser (FEL) is a coherent source of radiation in which the active medium consists of an ultrarelativistic electron beam moving in a periodic magnetic undulator. The alternating magnetic field forces the electrons to move along sinelike trajectories and, consequently, to emit radiation. The interaction between this optical field and the electron bunch may lead to an energy exchange and, as a consequence, to a coherent emission. After the recent success of the LEUTL [1] and TESLA-TTF [2] projects, single-pass devices, based on a self-amplified spontaneous emission (SASE) process, are now fully operational systems in the infrared-vacuum-ultraviolet spectral range. In the following, attention will be concentrated on the most usual FEL scheme, which employs an optical cavity where the radiation is stored and amplified on successive passes through the undulator. In this case, the electron-beam source is chosen for the desired laser performance: a LINAC [3] for a long-wavelength high power FEL or a storage ring for a visible or UV FEL [4]. If the accelerating system is provided by a radiofrequency (rf) field, the electron beam has a structure characterized by a series of microbunches with a separation fixed by the rf period. The stored light wave reproduces this time structure and consists of a train of short micropulses. A careful synchronization of the circulating micropulses and the electron bunches at each pass inside the optical cavity is required in order to achieve the laser oscillation. Due to their different velocity with respect to photon pulses, electrons slip back during their travel through the undulator by an amount $\Delta = N\lambda$, where λ is the radiation wavelength and N is the number of undulator periods. This slippage effect is characterized by the coupling parameter $\mu_c = \Delta/\sigma_\tau$ where σ_τ is the rms value associated with the longitudinal electron density profile. For relatively important values of μ_c, the reduced overlap with the ''gain medium'' leads to a significant reduction of the gain per pass that impedes the growth of the laser power. This effect is known as laser ''lethargy.'' Theoretical simulation and measurements done on the LINAC based FEL FELIX [5] (characterized by $\mu_c \simeq 10$) pointed out that the slippage effect dominates the laser dynamics leading to the simultaneous growth of different subpulses. The formation of ''spikes'' inside the FEL pulse has been also observed in LINAC based FELs characterized by smaller μ_c values [6] and on SASE devices (for which this phenomenon presents a systematic character [7]). In the latter case, a compensation scheme has been proposed [8], which is based on the so-called two-stage SASE FEL: two undulators and a monochromator located between them. The monochromator selects a narrow band from the SASE radiation coming out from the first undulator, which is then used as a seed for the second undulator.

The analysis that will be carried out in this paper concerns storage ring based FELs for which $\mu_c \ll 1$ (long electron bunch regime) and aims to highlight the conditions that can lead to a phenomenon similar to the mentioned one (even though based on a completely different mechanism), that is the growth of substructures inside the laser micropulse.

II. MICROPULSE STRUCTURE OF A STORAGE-RING FEL: THEORETICAL AND EXPERIMENTAL ANALYSES

Storage-ring FELs are characterized by a complex dynamics due to the fact that the laser pulse does not interact with a fresh electron bunch. As a consequence, the beam keeps the memory of successive interactions and the induced energy spread leads to saturation.

The optical pulse propagation in a storage-ring FEL has been analytically treated in Refs. [9,10,11], yielding important insight into the physical process. The laser electric field has been decomposed on a basis of longitudinal modes (the so-called ''supermodes'') self-reproducing in form after each round trip. After many round trips the system evolves towards the fundamental supermode characterized by a Gaussian profile. This approach is based on some important assumptions and the predicted results agree with measurements only in first approximation. In particular, the FEL gain modification is assumed to take place only through the reduction induced by the increase of the beam energy spread (inhomo-

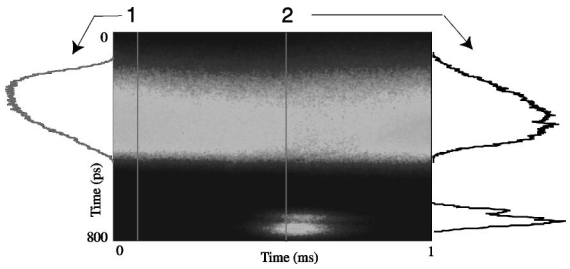

FIG. 1. Streak camera image of the super-ACO positron beam (upper image) and macropulse FEL (lower image). A vertical cut provides their longitudinal distribution while on the horizontal axis one can follow the evolution in time of the distribution profile. The FEL is operated in *Q*-switched mode, the pass-to-pass gain is about 2% and the cavity losses about 1%. Cut 1 is taken in the absence of the laser while cut 2 is taken after 130 μs from the beginning of the interaction. Super-ACO has been operated at 800 MeV with a current ranging between 90 and 25 mA (58 mA for the presented case) divided between two bunches and with two RF cavities. The full width at half maximum (FWHM) bunch width is about 350 ps. The FEL oscillates at 350 nm with an average power of 100 mW and presents a FWHM pulse duration of 70 ps.

geneous broadening) [10]; the shape of the longitudinal gain distribution is assumed to remain constantly Gaussian during the laser evolution. On the other hand, measurements done on the super-ACO FEL show that the electron-beam longitudinal profile (which is proportional to the gain) and the laser longitudinal profile may be non-Gaussian. As shown in Fig. 1, the FEL micropulse may present substructures and the electron-beam profile can be locally distorted. As we will see, these two effects are correlated and this implies that the coupling between the shapes of the laser-beam distributions plays an important role in determining the laser micropulse structure.

The presence of substructures inside the FEL micropulse was detected for the first time on the UVSOR FEL. In Ref. [12] a heuristic model is proposed that reduces their origin to an arbitrary internal structure already present in the spontaneous emission. In reality, as shown by numerical simulations done using the pass-to-pass tracking code we are going to introduce, this phenomenon can be traced back to the localized character of the laser-beam interaction that is due to the different size of their longitudinal distributions (the FEL distribution being much shorter).

The presented model considers the case of a storage-ring FEL implemented on an optical klystron, which consists of two undulators separated by a dispersive section (i.e., a strong magnetic field) favoring the interference between the emission of the two undulators [13,14]. Since the proper laser mode of the optical cavity is established after several hundred light paths, the longitudinal and transverse laser dynamics are assumed to be decoupled. The FEL-beam dynamics has been investigated by means of the three coupled equations:

$$\tau_{n+1} = \tau_n - \alpha T_0 \epsilon_n , \tag{1}$$

$$\begin{aligned}\epsilon_{n+1} = \epsilon_n + eV_{\mathrm{rf}}/E_0 \sin(\omega_{\mathrm{rf}}\tau_{n+1} + \phi) - U_{\mathrm{rad}}/E_0 - D(\epsilon_n, \tau_n) \\ + R(\epsilon_n, \tau_n) - r(\tau_n) + B\sqrt{I_n(\tau_n)}\sin(\omega_{\mathrm{las}}\tau_n + \psi) \\ - PI_n(\tau_n)\cos[4\pi(N+N_d)\epsilon_n],\end{aligned} \tag{2}$$

$$I_{n+1}(\tau_n) = R^2\{I_n(\tau_n - \delta\tau)[1 + G_n(\tau_n)] + i_s(\tau_n)\}, \tag{3}$$

where τ_n is the relative position of the electron at pass n with respect to the synchronous electron and ϵ_n its relative normalized energy; α is the momentum compaction and T_0 is the beam revolution period; ω_{rf} and V_{rf} are the frequency and the voltage of the rf cavity with associated phase ϕ; e is the electron charge, E_0 the nominal electron energy, U_{rad} the energy radiated per turn by synchrotron radiation, $D(\epsilon_n, \tau_n)$ the synchrotron damping term, $R(\epsilon_n, \tau_n)$ is associated with the stochastic process of photon emission [15]. The effect of the interaction of the electron beam with the ring environment is taken into account in Eq. (2) by the term $r(\tau_n)$ (which includes a first-order model of the ring impedance [16]). The FEL is characterized by the optical frequency ω_{las}, the relative phase ψ, and the intensity $I_n(\tau_n)$. The last two terms of Eq. (2) model the FEL-beam interaction and include the FEL induced microbunching and the energy lost by the electrons due to laser radiation. The bunching factor B depends on the FEL intensity, P is the FEL power, N the number of periods of the undulator, N_d is the interference order due to the dispersive section of the optical klystron. In Eq. (3), the seed of the normalized FEL distribution $I_n(\tau_n)$ is the spontaneous emission $i_s(\tau_n)$ and its evolution is determined by that of the gain $G_n(\tau_n)$ (whose profile coincides with that of the longitudinal beam distribution). The parameter R is the cavity mirror reflectivity, while $\delta\tau$ is a detuning parameter taking into account an eventual mismatch of the optical cavity length to the beam revolution period. Equation (3) is an approximate form of the FEL pulse propagation equation derived in Ref. [10]; it is, however, adequate for the present analysis. The FEL-beam longitudinal distributions are statistically determined by means of Eqs. (1)–(3). This model naturally applies to a FEL system, but it can be also used to study the interplay between an ultrarelativistic electron beam and an external laser in the case, for example, of generating femtosecond x-ray pulses [17].

Figure 2 shows the result of numerical simulations carried out for the case of the super-ACO FEL [18] operated in *Q*-switched mode at the perfect tuning [that is, $\delta\tau = 0$ in the Eq. (3)]. The experimental behavior of Fig. 1 is well reproduced. The interaction process can be described as following. The initial (FEL off) electron distribution is Gaussian [Fig. 2(a)]. During the laser rise time a deformation starts to become evident and finally a hole appears. The hole is the signature of the localized character of the interaction and is generated by the fact that electrons located around the center of the distribution interact on average for a longer period with the FEL than electrons at the edge, thus providing more energy to the laser. The consequent modulation of the gain profile is experienced by the FEL micropulse that subdivides in substructures growing in correspondence to the maxima of the beam distribution [see Fig. 2(b)]. The FEL macropulse

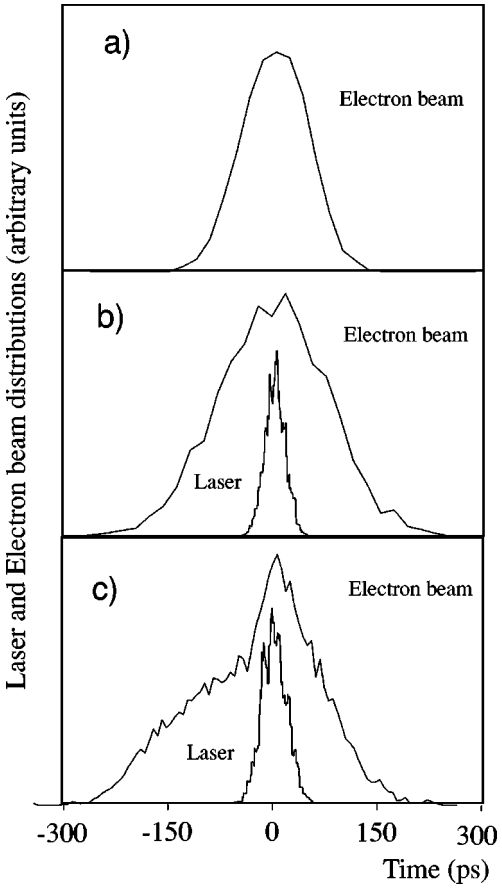

FIG. 2. Laser and beam longitudinal distributions statistically obtained by using Eqs. (1)–(3) for the case of the super-ACO FEL operated in *Q*-switched mode. (a) Initial (FEL off) electron distribution; (b) laser and beam longitudinal profiles after 130 μs from the beginning of the interaction. The simulation parameters have been chosen in agreement with the experimental conditions specified above; (c) the same as (b) except for the reduction of α by a factor of 1.5 with respect to its nominal value.

lasts for about 400 μs and after its decay electrons diffuse and the hole (observed for few tens of microseconds) disappears.

The distortion of the electron bunch distribution can be generally related to the ratio $r=\tau_{rise}/T_s$. T_s is the synchrotron oscillation period and τ_{rise} is the FEL rise time, which, for a generic laser system characterized by a gain G_0 and subject to the losses L, is given by $T_c/(G_0-L)$ (T_c is the period of the photons inside the optical cavity). The parameter r plays a role similar to the one of the parameter μ_c in LINAC based FELs. For a relatively small value of r the electrons can be considered as quasistatic during the growth of the FEL macropulse. As a consequence, the phase-space refreshing between successive interactions is modest, and a hole may appear in the electron distribution [19]. The localized character of the interaction is then enhanced and the substructures inside the FEL micropulse are more likely observed. Conversely, if r is relatively large, the FEL action during the growth of the macropulse is experienced by a large number of electrons and generally the beam distribution is heated, flattened but less locally distorted. In this case

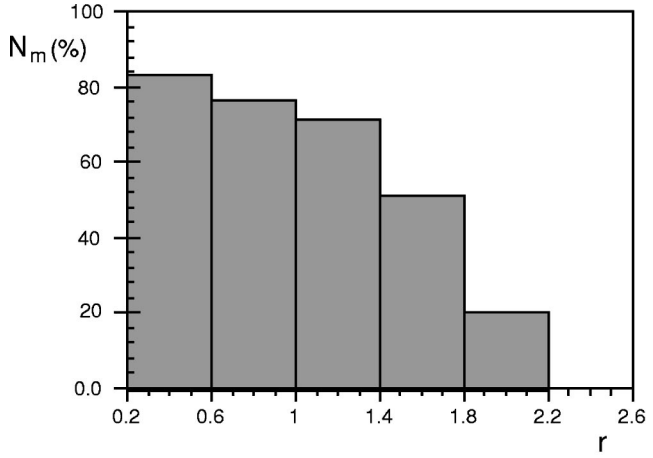

FIG. 3. Histogram of the probability of observing complex substructures inside the laser micropulse as a function of $r=\tau_{rise}/T_s$ for the case of the super-ACO FEL. T_s is measured using a spectral analyzer, τ_{rise} is deduced from the growth of the FEL intensity and the FEL substructures are detected by means of a double sweep streak camera in the beam current range 80–40 mA.

the laser micropulse profile is less perturbed and closer to a Gaussian distribution.

One of the electron-beam optics parameters controlling the factor r is the momentum compaction factor α. Because of the dependence of T_s on α, r is proportional to $\sqrt{\alpha}$. Figure 2(c) shows the numerical result obtained in the same condi-

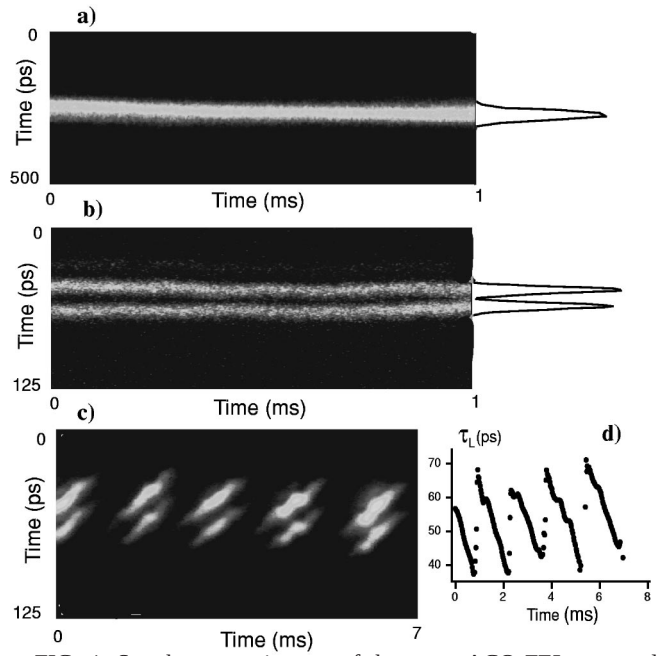

FIG. 4. Streak camera images of the super-ACO FEL operated in the natural mode. (a) cw FEL at the perfect tuning characterized by a nearly Gaussian profile; the FWHM pulse duration is about 40 ps. (b) cw FEL at the perfect tuning characterized by two separated substructures developing in parallel. (c) Pulsed FEL ($\delta\tau\simeq 20$ fs) characteriazed by substructures slipping inside the laser micropulse. (d) Position of the center of mass τ_L of the laser micropulse as a function of time for the case of (c).

tions of Fig. 2(b) (corresponding to $r=0.3$) but reducing α by a factor of 1.5. The beam distribution is more distorted by the laser onset and, as a consequence, the substructures inside the FEL micropulse become more evident.

In Fig. 3 the probability of observing complex substructures inside the laser micropulse is plotted as a function of r for the case of the super-ACO FEL. The variation range of r is determined by that of τ_{rise} and T_s with the beam current. The result is in agreement with theoretical simulations and shows that substructures are more often observed for smaller values of r. Simulations performed for the ELETTRA [20] and SOLEIL [21] FELs, which are characterized by a much smaller value of r ($r \simeq 7\times10^{-3}$ and $r \simeq 4\times10^{-3}$, respectively) with respect to super-ACO, show very evident distortions of the beam distributions and a systematic growth of several deep substructures in the laser pulse.

The FEL operated in Q-switched mode reaches high intracavity powers. In this case, the interaction between the laser-beam profiles is particularly strong and the FEL substructures are often observed. When the laser is operated in natural mode [18], its temporal distribution is normally Gaussian [see Fig. 4(a)]. However, although less frequently, substructures have been observed in the case of a cw FEL at the perfect tuning ($\delta\tau=0$) [see Fig. 4(b)] and in the case of a pulsed FEL [see Fig. 4(c)] obtained for $\delta\tau \simeq 20$ fs [22]. In the first case, the two substructures are completely separated and develop in parallel. In the second case they slip inside the micropulse with a drift speed imposed by the detuning (that is about 20 fs/pass); the FEL adopts a limit-cycle-type behavior [see Fig. 4(d)].

III. CONCLUSIONS

In this paper we have discussed the physical process inducing the growth of complex substructures inside the micropulse of a storage ring FEL (SRFEL). This phenomenon, which can be explained by a ''hole-burning-like'' process, is rather limited in the case of second generation SRFEL (such as super-ACO and UVSOR) if compared to the intrinsic spikes of a SASE pulse. Anyway, it can be expected to play an important role in the case of FELs installed on third generation storage rings, such as that of ELETTRA. The issue is particularly relevant for experiments that depend critically on the micropulse duration, for instance, in time-dependent spectroscopy.

[1] S. Milton *et al.*, Science (to be published).

[2] J. Rossbach, in *Proceedings of EPAC 2000* (Austrian Academy of Science Press, Virgina, 2000) http://www-hasylab.desy.de.

[3] T.J. Orzechowski *et al.*, Phys. Rev. Lett. **54**, 889 (1985).

[4] M. Billardon *et al.*, Phys. Rev. Lett. **51**, 1652 (1983).

[5] D.A. Jaroszynski *et al.*, Phys. Rev. Lett. **70**, 3412 (1993).

[6] R.W. Warren and J.C. Goldstein, Nucl. Instrum. Methods Phys. Res. A **272**, 155 (1988).

[7] R. Bonifacio *et al.*, Phys. Rev. Lett. **73**, 70 (1994).

[8] J. Feldhaus *et al.*, Opt. Commun. **140**, 341 (1997).

[9] P. Ellaume, IEEE J. Quantum Electron. **21**, 1012 (1985).

[10] G. Dattoli *et al.*, Phys. Rev. A **37**, 4326 (1988).

[11] G. Dattoli *et al.*, Phys. Rev. A **37**, 4334 (1988).

[12] H. Hama *et al.*, Nucl. Instrum. Methods Phys. Res. A **375**, 32 (1996).

[13] N.A. Vinokurov *et al.*, (unpublished).

[14] P. Elleaume, J. Phys. C **44**, 1 (1983).

[15] M. Sands, SLAC Report No. 121, 1970 (unpublished).

[16] R. Roux and M. Billardon, Nuovo Cimento Soc. Ital. Fis., A **112A**, 513 (1999).

[17] A.A. Zholents *et al.*, Phys. Rev. Lett. **76**, 912 (1983).

[18] R. Roux *et al.*, Phys. Rev. E **58**, 6584 (1998).

[19] G. De Ninno *et al.*, Phys. Rev. E **64**, 026502 (2001).

[20] R.P. Walker *et al.*, Nucl. Instrum. Methods Phys. Res. A **429**, 179 (1999).

[21] M.E. Couprie *et al.*, Nucl. Instrum. Methods Phys. Res. B **144**, 66 (1988).

[22] M.E. Couprie *et al.*, Phys. Rev. E **53**, 1871 (1996).